

# NJC

Accepted Manuscript



This is an *Accepted Manuscript*, which has been through the Royal Society of Chemistry peer review process and has been accepted for publication.

*Accepted Manuscripts* are published online shortly after acceptance, before technical editing, formatting and proof reading. Using this free service, authors can make their results available to the community, in citable form, before we publish the edited article. We will replace this *Accepted Manuscript* with the edited and formatted *Advance Article* as soon as it is available.

You can find more information about *Accepted Manuscripts* in the [Information for Authors](#).

Please note that technical editing may introduce minor changes to the text and/or graphics, which may alter content. The journal's standard [Terms & Conditions](#) and the [Ethical guidelines](#) still apply. In no event shall the Royal Society of Chemistry be held responsible for any errors or omissions in this *Accepted Manuscript* or any consequences arising from the use of any information it contains.

**Solution-processable two-dimensional conjugated organic  
small molecules containing triphenylamine core for  
photovoltaic application**

Leijing Liu,<sup>a</sup> Hui Li,<sup>a</sup> Ji Bian,<sup>a</sup> Jingyu Qian,<sup>a</sup> Yingjin Wei,<sup>b</sup> Jiyang Li,<sup>c</sup> and  
Wenjing Tian<sup>\*a</sup>

<sup>a</sup> *State Key Laboratory of Supramolecular Structure and Materials, Jilin University,  
Changchun 130012, P.R. China*

<sup>b</sup> *Key Laboratory of Physics and Technology for Advanced Batteries, Ministry of Education,  
Jilin University, Changchun 130012, P.R. China*

<sup>c</sup> *State Key Laboratory of Inorganic Synthesis and Preparative Chemistry, College of Chemistry,  
Jilin University, Changchun 130012, P.R. China*

**\*To whom all the correspondences should be addressed.**

Tel: +86-431-85166368

Fax: +86-431-85193421

E-mail: [wjtian@jlu.edu.cn](mailto:wjtian@jlu.edu.cn)

## Abstract

Two solution-processable two-dimensional conjugated organic small molecules based on triphenylamine (TPA) core, **TPA-BT-C8** and **TPA-3Th**, were designed and synthesized. As to **TPA-BT-C8**, two arms of TPA core are symmetrically connected with thiophene donor group and benzothiadiazole acceptor group, while the third arm consists of a strong acceptor group of 2-(5,5-dimethylcyclohex-2-en-1-ylidene)malononitrile (DCM) connected through a *trans* double bond with TPA core. For **TPA-3Th**, two arms of its TPA core are composed of only donor group, terthiophene, whereas the third arm consists of an acceptor group of cyano-*n*-octyl acetate connected through a *trans* double bond with TPA core. The investigation indicated that **TPA-BT-C8** has a lower energy band gap and wider absorption than **TPA-3Th** due to the strong intramolecular charge transfer effect in **TPA-BT-C8**. The two molecules have a deep highest occupied molecular orbital (HOMO) energy level. Bulk heterojunction photovoltaic devices were fabricated using **TPA-BT-C8** or **TPA-3Th** as donor and (6,6)-phenyl C<sub>61</sub>-butyric acid methyl ester (PCBM) as acceptor. All the devices have a high open-circuit voltage ( $V_{oc}$ ) of about 0.9 eV. Device based on **TPA-BT-C8** has a much higher short circuit current ( $J_{sc}$ ) (8.47 mA cm<sup>-2</sup>) and power conversion efficiency (PCE) (2.26%) than device based on **TPA-3Th** (4.32 mA cm<sup>-2</sup>, 1.21%), resulting from wider solar light absorption of **TPA-BT-C8** and better compatibility and film-formation ability of **TPA-BT-C8** with PCBM than **TPA-3Th**. Incident photon-to-electron conversion efficiency (IPCE) spectra also confirmed that **TPA-BT-C8** based device has a wider

and red-shifted response range than **TPA-3Th** based device, which leads to a higher performance of the former device.

## Introduction

Bulk-heterojunction organic solar cells (OSCs) have been receiving a great deal of attention in recent years due to their advantages of low cost, light weight and capability to be fabricated into flexible devices.<sup>1</sup> In comparison with conjugated polymers, solution-processable organic small molecules possess the advantages of high purity, definite molecular weight, simple purification and better batch-to-batch reproducibility for the application in bulk-heterojunction OSCs. Therefore, solution-processable organic small molecules have drawn considerable interest and achieved great progress in recent years in OSCs.<sup>2</sup>

TPA unit possesses a three-dimensional propeller structure, which makes the TPA containing molecules exhibit good solution processability. Moreover, TPA is a strong electron-donor unit and has a good charge transport ability, and accordingly the TPA derivatives have high hole mobility and are widely used as hole-transporting materials in organic light-emitting diodes (OLEDs),<sup>3</sup> sensitizers in dye-sensitized solar cells (DSSCs)<sup>4</sup> and photovoltaic cells.<sup>3b,5,6</sup> Yongfang Li group synthesized many star-shaped D- $\pi$ -A structural molecules containing TPA as the core and different acceptor units or a combination of acceptor units and donor units as arms, and they applied these molecules in organic photovoltaic devices as donor materials.<sup>6,7</sup> Jean Roncali group developed some star-shaped TPA  $\pi$ -conjugated systems with internal charge-transfer (ICT) and used them as donor materials for heterojunction solar cells.<sup>8</sup>

In addition, other research groups also reported some star-shaped molecules based on TPA core for photovoltaic applications.<sup>5d,9</sup> However, it is worth noting that for all of these reported TPA derivatives, their three arms are constructed by the same molecular structures or at least part of their three arms are the same. This more or less brings about some limitations to tune the photophysical properties, energy level and photovoltaic properties of the molecules.

Alex K.-Y. Jen group reported two conjugated two-dimensional copolymers PFDCN and PFPDT with donor- $\pi$ -bridge-acceptor side chains,<sup>10</sup> which takes advantage of nonlinear optical chromophores to optimize the absorption spectra and energy levels of the resultant polymers,<sup>11</sup> and the two-dimensional conjugated structure of these polymers may improve their isotropic charge transport.<sup>12</sup> Resultantly, both of the two copolymers exhibit excellent photovoltaic properties.

Herein, we designed and synthesized two novel solution-processable two-dimensional conjugated organic small molecules, (E)-2-(3-(4-(Bis(4-(7-(5-octylthiophen-2-yl)benzo[c][1,2,5]thiadiazol-4-yl)phenyl)amino)styryl)-5,5-dimethylcyclohex-2-en-1-ylidene)malononitrile (**TPA-BT-C8**) and (E)-Octyl-3-(4-(bis(4-([2,2':5',2''-terthiophen]-5-yl)phenyl)amino)phenyl)-2-cyanoacrylate (**TPA-3Th**) (Scheme 1) by using TPA based structure. Different from the common linear or star-shaped TPA derivatives, in **TPA-BT-C8** and **TPA-3Th**, two arms of TPA core are symmetrically connected with donor and acceptor or just donor groups, while the third arm is connected with different electron-withdrawing groups through a *trans* double bond. The results indicated that both of the two molecules has

a deep HOMO energy level, and **TPA-BT-C8** has a lower energy band gap and wider solar light absorption than **TPA-3Th**. Bulk heterojunction photovoltaic devices were fabricated using **TPA-BT-C8** or **TPA-3Th** as donor and PCBM as acceptor. Both of the two devices have a high  $V_{oc}$ . The device based on **TPA-BT-C8** has a higher  $J_{sc}$  and PCE than the device based on **TPA-3Th**.

## Experimental section

### Materials

Potassium acetate, [1,1'-Bis(diphenylphosphino)ferrocene]dichloropalladium(II) ( $\text{PdCl}_2(\text{dppf})$ ), Bis(triphenylphosphine)palladium(II) chloride ( $\text{PdCl}_2(\text{PPh}_3)_2$ ), Tetrakis(triphenylphosphine)palladium ( $\text{Pd}(\text{PPh}_3)_4$ ) and n-octyl cyanoacetate were purchased from J&K Company. Butyl lithium was got from Acros. Piperidine was purchased from Shanghai Chemical Reagent Company. Dichloromethane, dioxane, chloroform and acetonitrile were got from Beijing Chemical Reagent Company. The other reagents and solvents were purchased from Tianjin Tiantai Chemical Reagent Company. All reagents and chemicals were used without further purification unless stated otherwise.

### Instruments

$^1\text{H}$  NMR and  $^{13}\text{C}$  NMR spectra were measured using a Bruker AVANCE-500 NMR spectrometer spectrometer and a Varian Mercury-300 NMR, respectively. The elemental analysis was carried out with an American PERKIN ELMER 2400LS II CHNS-Ovelemental analyzer. The mass spectra were recorded on a Kratos

MALDI-TOF mass system. Thermogravimetric analysis (TGA) were performed on a Perkin-Elmer Pyris 1 analyzer under a nitrogen atmosphere ( $100 \text{ mL min}^{-1}$ ) at a heating rate of  $10 \text{ }^\circ\text{C min}^{-1}$ . UV-visible absorption spectra were measured using a Shimadzu UV-3000 spectrophotometer. Electrochemical measurements were performed with a Bioanalytical Systems BAS 100 B/W electrochemical workstation. Atomic force microscope (AFM) morphology was scanned with the Nanoscope IIIa Dimension 3100 atomic force microscopy.

## Synthesis

Compound **1** was synthesized following the procedures in Ref.,<sup>13</sup> and Tributyl(5-octylthiophen-2-yl)stannane and 2,2':5',2''-terthiophene were synthesized following the procedures in Ref.<sup>14</sup>

### **4-(bis(4-(4,4,5,5-tetramethyl-1,3,2-dioxaborolan-2-yl)phenyl)amino)benzaldehyde (2)**

In a two-necked round bottom flask, compound **1** (2.15 g, 5 mmol), Bis(pinacolato)diboron (3.81 g, 15 mmol), potassium acetate (3.93 g, 40 mmol) and  $\text{PdCl}_2(\text{dppf})$  (0.12 g, 0.15 mmol) were dissolved in 50 mL of dioxane, and the mixture was heated to  $80 \text{ }^\circ\text{C}$ , stirred for 8 h and the reaction was finished. Then the reaction mixture was cooled to room temperature and poured into 300 mL of ice water, and extracted using dichloromethane ( $3 \times 300 \text{ mL}$ ). The organic phase was dried over anhydrous magnesium sulfate ( $\text{MgSO}_4$ ), and then the solvent was removed using a rotary evaporator. The crude product was purified by column chromatography using a cosolvent (petroleum ether/ethyl acetate, 5:1 V/V) as the eluent to give 2 g of white

solid with a yield of 76%.  $^1\text{H}$  NMR (300 MHz,  $\text{CDCl}_3$ , TMS):  $\delta$ (ppm) 9.84 (s, 1H), 7.76 (d,  $J = 8.7$  Hz, 4H), 7.71 (d,  $J = 8.7$  Hz, 2H), 7.14 (d,  $J = 8.7$  Hz, 4H), 7.11 (d,  $J = 8.7$  Hz, 2H), 1.35 (s, 24H).

**4-Bromo-7-(5-octylthiophen-2-yl)benzo[c][1,2,5]thiadiazole (3).** In a one-necked round bottom flask under nitrogen, tributyl(5-octylthiophen-2-yl)stannane (0.5 g, 1.03 mmol) and 4,7-dibromobenzo[c][1,2,5]thiadiazole (0.5 g, 1.7 mmol),  $\text{PdCl}_2(\text{PPh}_3)_2$  (10 mg) were dissolved in 70 mL of tetrahydrofuran (THF). The mixture was heated to 60 °C, and stirred overnight at this temperature. Then the reactant was cooled to room temperature, and the solvent was removed using a rotary evaporator. The crude product was purified by column chromatography using a cosolvent (petroleum ether/dichloromethane, 10:1 V/V) as the eluent to give 0.3 g of orange solid with a yield of 71%.  $^1\text{H}$  NMR (300 MHz,  $\text{CDCl}_3$ , TMS):  $\delta$ (ppm) 7.91 (d,  $J = 3.7$  Hz, 1H), 7.80 (d,  $J = 7.7$  Hz, 1H), 7.62 (d,  $J = 7.7$  Hz, 1H), 6.87 (d,  $J = 3.7$  Hz, 1H), 2.89 (t,  $J = 7.6$  Hz, 2H), 1.76 (m, 2H), 1.28 (m, 10H), 0.88 (t, 3H).  $^{13}\text{C}$  NMR (75 MHz,  $\text{CDCl}_3$ , TMS):  $\delta$ (ppm) 153.73, 151.73, 148.52, 135.77, 132.24, 128.01, 127.39, 125.33, 125.02, 111.47, 31.83, 31.56, 30.27, 29.31, 29.20, 29.12, 22.64, 14.10.

**4-(Bis(4-(7-(5-octylthiophen-2-yl)benzo[c][1,2,5]thiadiazol-4-yl)phenyl)amino)**

**benzaldehyde (4).** In a one-necked round bottom flask under nitrogen, a mixture of compound **2** (0.3 g, 0.57 mmol), compound **3** (0.3 g, 0.57 mmol),  $\text{Pd}(\text{PPh}_3)_4$  (0.033 g), 4 mL of solution of sodium carbonate in water ( $\text{Na}_2\text{CO}_3$ ) (2 M) and 6 mL of toluene was heated to reflux for 24 h under stirring. Then the reactant was cooled to room temperature, and poured into 100 mL of water, and extracted using dichloromethane

(3×110 mL). The organic phase was dried over anhydrous MgSO<sub>4</sub>, and then the solvent was removed using a rotary evaporator. The crude product was purified by column chromatography using a cosolvent (petroleum ether/ethyl acetate, 10:1 V/V) as the eluent to give 0.48 g of red solid with a yield of 90%. <sup>1</sup>H NMR (300 MHz, CDCl<sub>3</sub>, TMS): δ(ppm) 9.88 (s, 1H), 8.02 (t, *J* = 6.3 Hz, 6H), 7.90 (d, *J* = 7.5 Hz, 2H), 7.79 (d, *J* = 8.8 Hz, 2H), 7.75 (d, *J* = 7.5 Hz, 2H), 7.41 (d, *J* = 8.7 Hz, 4H), 7.29 (d, *J* = 8.7 Hz, 2H), 6.91 (d, *J* = 3.7 Hz, 2H), 2.93 (t, *J* = 7.6 Hz, 4H), 1.77 (m, 4H), 1.29 (m, 20H), 0.90 (t, 6H), <sup>13</sup>C NMR (75 MHz, CDCl<sub>3</sub>, TMS): δ(ppm) 190.35, 152.59, 148.03, 146.47, 145.88, 136.54, 133.92, 132.22, 131.26, 130.37, 127.83, 127.64, 125.89, 125.68, 125.19, 124.99, 121.06, 31.79, 31.56, 30.24, 29.27, 29.15, 29.10, 22.59, 14.04.

**2-([2,2':5',2''-Terthiophen]-5-yl)-4,4,5,5-tetramethyl-1,3,2-dioxaborolane (5).** In a three-necked round bottom flask under nitrogen, 2,2':5',2''-terthiophene (1 g, 4 mmol) was dissolved in 50 mL of THF. The mixture was cooled to -78 °C and stirred. Then 1.8 mL of solution of butyl lithium in hexane (2.4 M) was slowly dropped into the flask, and the reactant was warmed to -40 °C, stirred at this temperature for 2 h. The mixture was cooled to -78 °C again, and isopropoxyboronic acid pinacol ester (0.9 mL) was added. The reaction mixture was warmed to room temperature, stirred overnight, and then poured into 150 mL of water, and extracted using dichloromethane (3×130 mL). The organic phase was dried over anhydrous MgSO<sub>4</sub>, and then the solvent was removed using a rotary evaporator. The crude product was purified by column chromatography using a cosolvent (petroleum ether/ethyl acetate, 10:1 V/V) as the

eluent to give 0.96 g of green solid with a yield of 64%.  $^1\text{H}$  NMR (300 MHz,  $\text{CDCl}_3$ , TMS):  $\delta(\text{ppm})$  7.54 (d,  $J = 3.6$  Hz, 1H), 7.24 (d,  $J = 3.6$  Hz, 1H), 7.22 (d,  $J = 3.6$  Hz, 1H), 7.19 (dd,  $J = 3.6$  Hz,  $J = 1.2$  Hz, 1H), 7.15 (d,  $J = 3.8$  Hz, 1H), 7.09 (d,  $J = 3.8$  Hz, 1H), 7.03 (dd,  $J = 5.1$  Hz,  $J = 3.6$  Hz, 1H), 1.36 (s, 12H).  $^{13}\text{C}$  NMR (75 MHz,  $\text{CDCl}_3$ , TMS):  $\delta(\text{ppm})$  137.89, 127.81, 124.92, 124.79, 124.56, 124.40, 123.81, 84.15, 24.72.

**4-(Bis(4-([2,2':5',2''-terthiophen]-5-yl)phenyl)amino)benzaldehyde (6).** In a one-necked round bottom flask under nitrogen, a mixture of compound **2** (107 mg, 0.25 mmol), compound **5** (253 mg, 0.68 mmol),  $\text{Pd}(\text{PPh}_3)_4$  (15 mg), 2 mL of solution of  $\text{Na}_2\text{CO}_3$  in water (2 M) and 3 mL of toluene was heated to reflux for 24 h under stirring. Then the reactant was cooled to room temperature, and poured into 50 mL of water, and extracted using dichloromethane ( $3 \times 60$  mL). The organic phase was dried over anhydrous  $\text{MgSO}_4$ , and then the solvent was removed using a rotary evaporator. The crude product was purified by column chromatography using dichloromethane as the eluent to give 0.13 g of yellow solid with a yield of 68%.  $^1\text{H}$  NMR (300 MHz,  $\text{CDCl}_3$ , TMS):  $\delta(\text{ppm})$  9.86 (s, 1H), 7.76 (d,  $J = 8.9$  Hz, 2H), 7.58 (d,  $J = 8.8$  Hz, 4H), 7.20 (m, 18H), 7.05 (dd,  $J = 5.1$  Hz,  $J = 3.6$  Hz, 2H),  $^{13}\text{C}$  NMR (75 MHz,  $\text{CDCl}_3$ , TMS):  $\delta(\text{ppm})$  190.30, 145.36, 131.30, 130.81, 130.09, 128.81, 127.85, 126.83, 126.15, 124.60, 124.54, 124.38, 124.22, 123.75, 120.67.

**(E)-2-(3-(4-(Bis(4-(7-(5-octylthiophen-2-yl)benzo[c][1,2,5]thiadiazol-4-yl)phenyl)amino)styryl)-5,5-dimethylcyclohex-2-en-1-ylidene)malononitrile (TPA-BT-C8).** In a two-necked round bottom flask under nitrogen, a mixture of compound **4** (130 mg,

0.14 mmol), acetonitrile (6 mL), piperidine (10 drops) and 2-(5,5-dimethylcyclohex-2-en-1-ylidene)malononitrile (39 mg) were heated to reflux for 24 h. Then the reactant was cooled to room temperature, and the solvent was removed using a rotary evaporator. The crude product was purified by column chromatography using a cosolvent (petroleum ether/dichloromethane, 1:1 V/V) as the eluent to give 110 mg of red solid with a yield of 72%. <sup>1</sup>H NMR (300 MHz, CDCl<sub>3</sub>, TMS): δ(ppm) 7.98 (m, 6H), 7.88 (d, *J* = 7.5 Hz, 2H), 7.73 (d, *J* = 7.5 Hz, 2H), 7.46 (d, *J* = 8.7 Hz, 2H), 7.37 (d, *J* = 8.7 Hz, 4H), 7.25 (d, *J* = 8.7 Hz, 2H), 7.07 (d, *J* = 16.2 Hz, 1H), 6.93 (d, *J* = 16 Hz, 1H), 6.90 (d, *J* = 3.9 Hz, 2H), 6.82 (s, 1H), 2.92 (t, *J* = 7.6 Hz, 4H), 2.60 (s, 2H), 2.47 (s, 2H), 1.76 (m, 4H), 1.29 (m, 20H), 1.06 (s, 6H), 0.89 (t, 6H). <sup>13</sup>C NMR (75 MHz, CDCl<sub>3</sub>, TMS): δ(ppm) 168.97, 154.10, 153.89, 152.85, 148.77, 147.95, 146.65, 136.71, 136.59, 132.88, 131.27, 130.19, 129.93, 128.82, 127.61, 127.35, 126.65, 125.19, 125.11, 124.91, 123.37, 122.81, 113.65, 112.90, 77.76, 43.01, 39.31, 31.97, 31.82, 31.59, 30.28, 29.64, 29.30, 29.17, 27.99, 22.60, 14.01. MALDI-TOF MS calcd for C<sub>67</sub>H<sub>67</sub>N<sub>7</sub>S<sub>4</sub> 1098.44; found 1099.44.

**(E)-Octyl-3-(4-(bis(4-([2,2':5',2''-terthiophen]-5-yl)phenyl)amino)phenyl)-2-cyanoacrylate (TPA-3Th).** In a two-necked round bottom flask under nitrogen, a mixture of compound **6** (70 mg, 0.09 mmol), n-octyl cyanoacetate (0.18 μL, 0.09 mmol), triethylamine (0.15 mL) and chloroform (5 mL) were heated to reflux for 24 h. Then the reactant was cooled to room temperature, and the solvent was removed using a rotary evaporator. The crude product was purified by column chromatography using a cosolvent (petroleum ether/dichloromethane, 2:1 V/V) as the eluent to give 60 mg of

orange solid with a yield of 71%.  $^1\text{H}$  NMR (300 MHz,  $\text{CDCl}_3$ , TMS):  $\delta$ (ppm) 8.11 (s, 1H), 7.91 (d,  $J = 8.7$  Hz, 2H), 7.59 (d,  $J = 8.7$  Hz, 4H), 7.21 (m, 18H), 7.05 (m, 2H), 4.31 (t,  $J = 6.6$  Hz, 2H), 2.06 (m, 2H), 1.75 (m, 2H), 1.26 (m, 8H), 0.89 (t, 3H).  $^{13}\text{C}$  NMR (75 MHz,  $\text{CDCl}_3$ , TMS):  $\delta$ (ppm) 163.50, 162.88, 153.64, 151.61, 144.96, 142.29, 137.10, 136.55, 136.41, 136.11, 133.10, 131.11, 127.89, 126.90, 126.34, 124.66, 124.58, 124.41, 124.28, 123.89, 123.79, 120.47, 67.12, 31.71, 29.07, 28.34, 25.68, 24.67, 22.58, 14.00. MALDI-TOF MS calcd for  $\text{C}_{54}\text{H}_{44}\text{N}_2\text{O}_2\text{S}_6$  944.17; found 945.18.

### Photovoltaic device fabrication and characterization

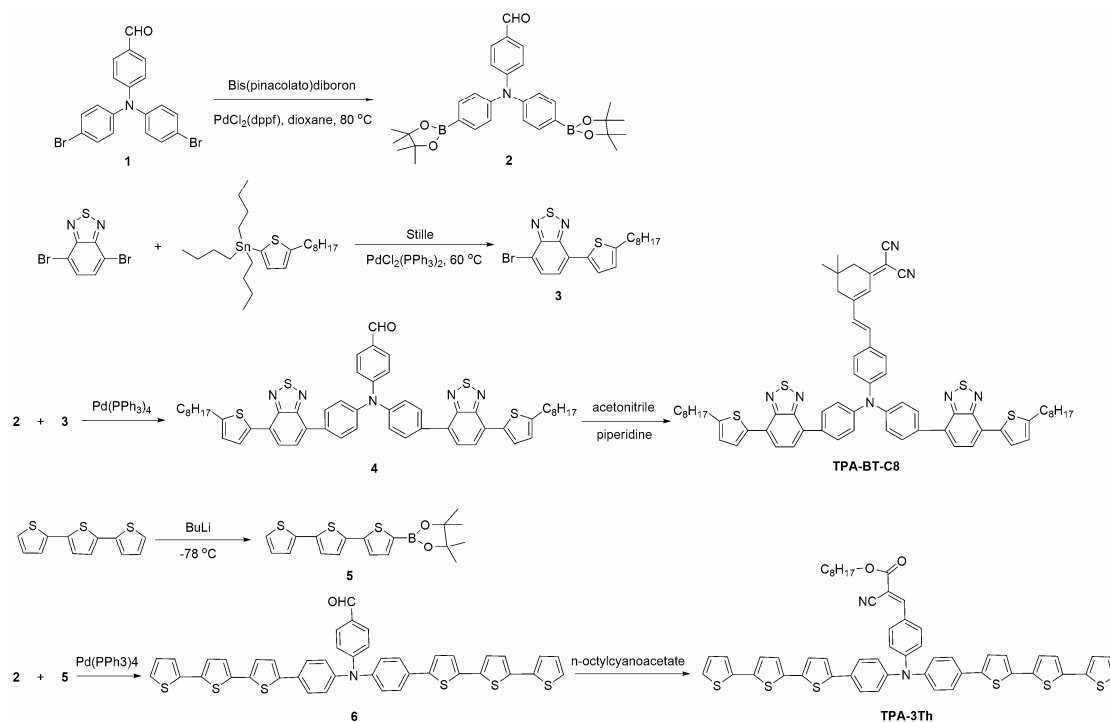
Mixed solutions for the active film and morphology investigation were prepared by dissolving **TPA-BT-C8**:PCBM and **TPA-3Th**:PCBM in the solvent of chlorobenzene with the blend ratios of 1:1, 1:2.5 and 1:3, respectively, then continuously stirring overnight at 40 °C. The bulk heterojunction photovoltaic devices were prepared as follows: The ITO-covered glass substrate was used as the anode in the devices. It was cleaned in an ultrasonic bath with detergent, chloroform, acetone and isopropyl alcohol in turn. Then the substrates were treated in an oxygen plasma cleaner for about 5 min. Subsequently, PEDOT:PSS was spin-coated from an aqueous dispersion onto the cleaned ITO substrate to form a thin film with a thickness of about 50 nm. The active layer was prepared by spin-coating on top of the PEDOT:PSS layer, and the thickness was around 73 nm. Finally, the cathode of LiF/Al about 100 nm was deposited by thermal evaporation in a vacuum chamber under the pressure of  $5 \times 10^{-4}$  Pa. The effective photovoltaic area as defined by the geometrical overlap between the

bottom ITO electrode and the top cathode was 4 mm<sup>2</sup>. The current-voltage (*I-V*) characteristics were measured with a computer-controlled Keithley 2400 Source Meter Measurement System in the dark or under 100 mW cm<sup>-2</sup> illumination from a Sciencetech 500-W solar simulator (AM 1.5G). The class of Sciencetech 500-W solar simulator (AM 1.5G) is A.

## Results and discussion

### Synthesis and characterization

The synthesis procedures of the two-dimensional conjugated organic small molecules, **TPA-BT-C8** and **TPA-3Th**, are depicted in scheme 1. Compound **3** was synthesized via Stille reaction, and compound **4** and **6** were synthesized via Suzuki reaction. Compound **5** was synthesized from isopropoxyboronic acid pinacol ester and lithiated 2,2':5',2''-terthiophene at -78 °C. The final molecules **TPA-BT-C8** and **TPA-3Th** were synthesized via Knoevenagel condensation reaction. The chemical structures of the compounds were confirmed by <sup>1</sup>H NMR and <sup>13</sup>C NMR spectra. The double peaks of coupling constant *J*~16 in <sup>1</sup>H NMR spectra indicate that the double bond presents a *trans* configuration. in **TPA-BT-C8**. The characteristic peak of aldehyde group at the chemical shift of 10.0 ppm in <sup>1</sup>H NMR spectrum of compound **6** disappears in that of **TPA-3Th**, while a single peak at the chemical shift of 8.114 ppm appears, which indicates that the *trans* double bond forms in **TPA-3Th**. Both **TPA-BT-C8** and **TPA-3Th** exhibit good solubility in common organic solvents such as chloroform, dichloromethane and chlorobenzene etc. at room temperature.



Scheme 1 Synthetic route of TPA-BT-C8 and TPA-3Th.

### Thermal properties

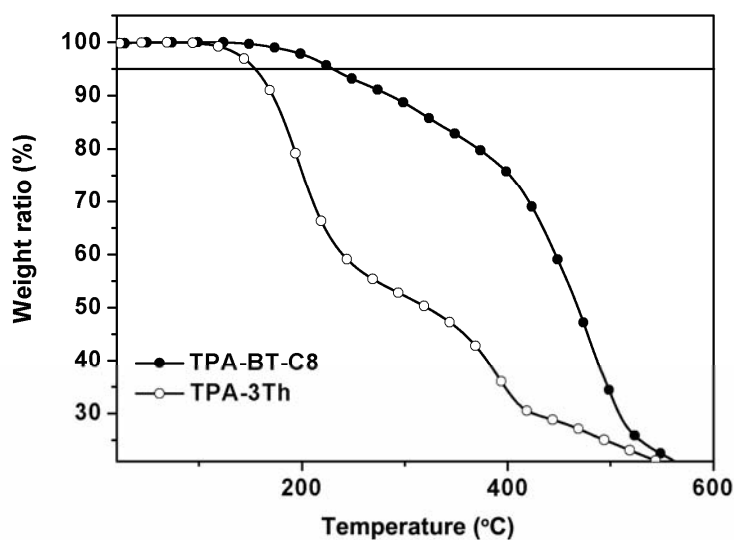


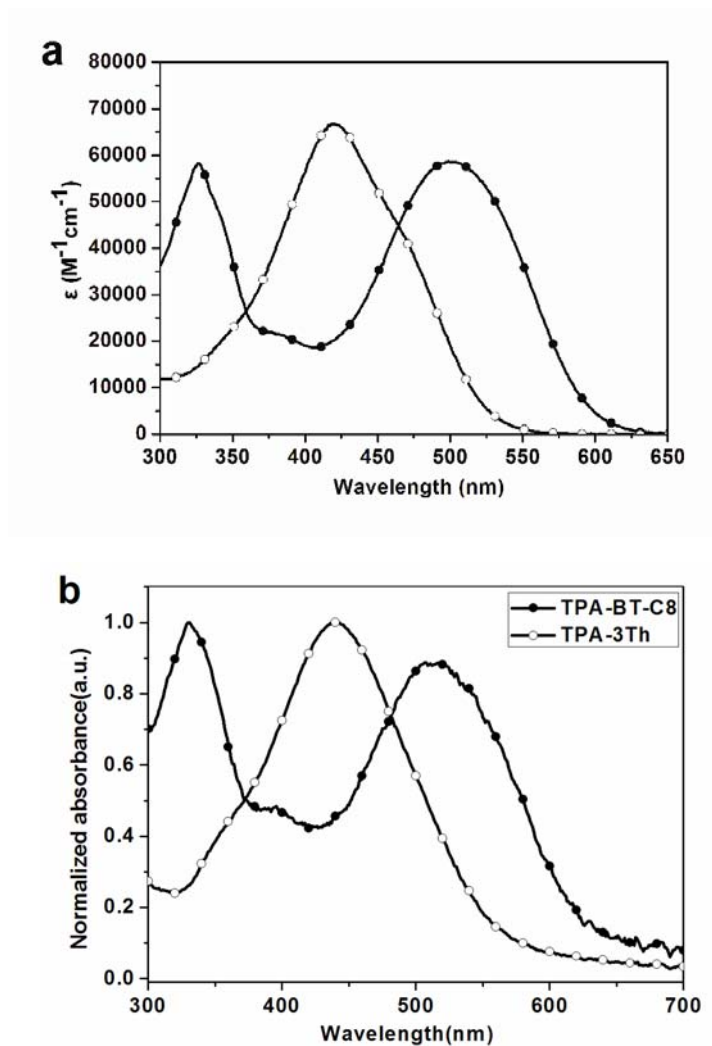
Fig. 1 TGA curves of TPA-BT-C8 and TPA-3Th at a heating rate of 10 °C min<sup>-1</sup> under the protection of nitrogen.

Fig. 1 shows the TGA curves of TPA-BT-C8 and TPA-3Th scanned at a heating rate of 10 °C min<sup>-1</sup> under the protection of nitrogen. The 5% weight-loss temperature

( $T_d$ ) of **TPA-BT-C8** is at 227 °C, much higher than that of **TPA-3Th** which is at 153 °C. As for low molecular weight materials, the  $T_d$  of **TPA-BT-C8** and **TPA-3Th** is high enough for photovoltaic device application.

### Optical properties

The normalized UV-vis absorption spectra of **TPA-BT-C8** and **TPA-3Th** in dilute chloroform solution ( $10^{-5}$  M) and in solid thin film are shown in Fig. 2. The relevant spectroscopic data of the two small molecules are summarized in Table 1. In dilute chloroform solution, **TPA-BT-C8** exhibit two parts of absorption, a relative narrow absorption band with a peak at 329 nm and a wide absorption band with a maximum at 500 nm, which can be assigned to the intramolecular  $\pi$ - $\pi^*$  transition and the ICT interaction between the electron-donor and acceptor groups, respectively. As to **TPA-3Th**, it has no electron-acceptor group in the main chain except a weak cyano acrylate group in the third arm, so there is only a weak ICT band resulting from a somewhat smaller charge transfer from TPA to the cyano acrylate group. Moreover, the absorption band with a peak at 420 nm and a weakly discernible shoulder observed for **TPA-3Th** should correspond to the addition of a  $\pi$ - $\pi^*$  transition and the weak ICT band. Both of the two compounds have a relatively high molar absorption coefficient, which is  $6.0 \times 10^4 \text{ M}^{-1} \text{ cm}^{-1}$  for **TPA-BT-C8** and  $6.7 \times 10^4 \text{ M}^{-1} \text{ cm}^{-1}$  for **TPA-3Th** calculated by Lambert-Beer's law.<sup>15</sup>



**Fig. 2** Absorption spectra of **TPA-BT-C8** and **TPA-3Th** in chloroform solution with concentration of  $10^{-5} \text{ mol L}^{-1}$  (a) and in thin solid film (b).

**Table 1** Summary of optical physical and electrochemical properties of **TPA-BT-C8** and **TPA-3Th**.

Molecule	$\lambda_{\text{max}}^{\text{abs } a}$ (nm)	$\lambda_{\text{max}}^{\text{abs } b}$ (nm)	$E_{\text{g}}^{\text{opt } c}$ (eV)	$E_{\text{ox}}^{\text{onset}}$ (V)	HOMO (eV)	$E_{\text{red}}^{\text{onset}}$ (V)	LUMO (eV)	$E_{\text{g}}^{\text{el}}$ (eV)
<b>TPA-BT-C8</b>	329, 500	330, 517	1.98	0.68	-5.38	-1.13	-3.57	1.81
<b>TPA-3Th</b>	420	438	2.21	0.65	-5.35	-1.20	-3.50	1.85

<sup>a</sup> In chloroform ( $1 \times 10^{-5} \text{ M}$ )

<sup>b</sup> In thin solid film

<sup>c</sup>  $E_{\text{g}}^{\text{opt}} = 1240/\lambda_{\text{edge}}^{\text{film}}$

Compared with the absorption spectra in dilute chloroform solution, the absorption spectra of **TPA-BT-C8** and **TPA-3Th** in solid film have a red shift of  $\sim 20$

nm. Because the three-dimensional structure of TPA restrains the  $\pi$ - $\pi$  stacking effect of **TPA-BT-C8** and **TPA-3Th**, so the red shift in solid state is not so high as other molecules. The maximum absorption peak of **TPA-BT-C8** is at 330 nm, indicating that in thin solid film, the  $\pi$ - $\pi^*$  transition absorption is dominant, not like in dilute solution, the  $\pi$ - $\pi^*$  transition absorption and ICT interaction absorption are comparable. According to the onset of the optical absorption in thin film, the optical band gap ( $E_g^{\text{opt}}$ ) of **TPA-BT-C8** and **TPA-3Th** is estimated to be 1.98 eV and 2.21 eV, respectively.

### Electrochemical properties

The electrochemical properties of **TPA-BT-C8** and **TPA-3Th** were investigated by cyclic voltammetry (CV). The measurements were carried out in anhydrous acetonitrile under the protection of nitrogen, using platinum button as working electrode, Ag/AgNO<sub>3</sub> as reference electrode, platinum wire as counter electrode, and tetrabutylammonium hexafluorophosphate (TBAPF<sub>6</sub>, 0.1 mol L<sup>-1</sup>) as supporting electrolyte. Ferrocene was used as the internal standard and showed a peak at +0.1 V versus Ag/Ag<sup>+</sup>. The CV curves are shown in Fig. 3, and the electrochemical parameters are summarized in Table 1. It can be found that **TPA-BT-C8** and **TPA-3Th** exhibit semi-reversible redox behavior. The onset oxidation potential ( $E_{\text{ox}}^{\text{onset}}$ ) and onset reduction potential ( $E_{\text{red}}^{\text{onset}}$ ) of **TPA-BT-C8** are at ca. 0.68 and -1.13 V respectively, and for **TPA-3Th**, they are at 0.65 and -1.20 V. From  $E_{\text{ox}}^{\text{onset}}$  and  $E_{\text{red}}^{\text{onset}}$  of **TPA-BT-C8** and **TPA-3Th**, their HOMO and lowest unoccupied molecular orbital (LUMO) energy level as well as electrochemical energy band gap

( $E_g^{el}$ ) can be calculated according to the following equations:<sup>16</sup>

$$\text{HOMO (eV)} = -e(E_{\text{ox}}^{\text{onset}} + 4.7 \text{ V})$$

$$\text{LUMO (eV)} = -e(E_{\text{red}}^{\text{onset}} + 4.7 \text{ V})$$

$$E_g^{el} = -(\text{HOMO} - \text{LUMO}) \text{ (eV)}$$

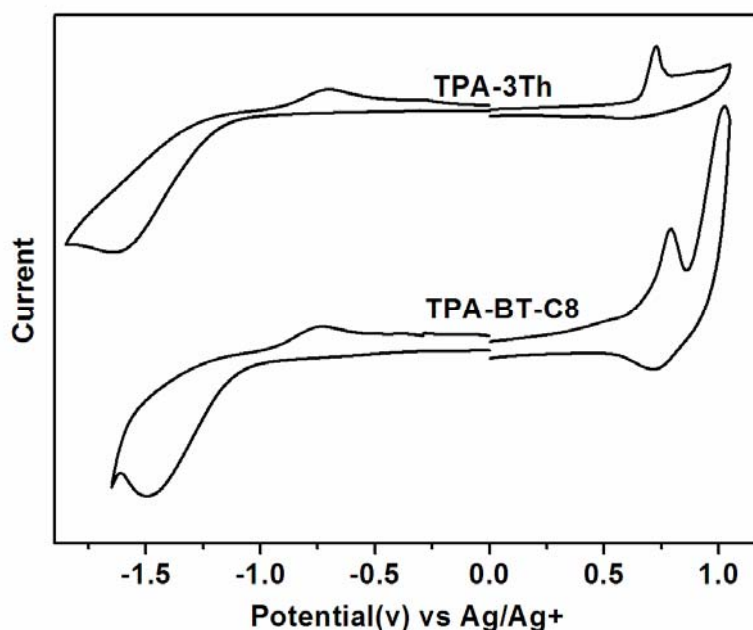


**Fig. 3** Cyclic voltammety curves of **TPA-BT-C8** and **TPA-3Th** films on platinum electrode in 0.1 mol L<sup>-1</sup> acetonitrile solution of TBAPF<sub>6</sub> at a scan rate of 100 mV s<sup>-1</sup>.

The HOMO and LUMO energy levels as well as the electrochemical band gap of **TPA-BT-C8** are -5.38, -3.57 and 1.81 eV, and as to **TPA-3Th**, they are -5.35, -3.50 and 1.85 eV. It can be found that the two molecules have a deep HOMO energy level, far below the air oxidation threshold (ca. -5.2 eV),<sup>17</sup> which ensures a good air stability of the molecules and allows a high  $V_{oc}$  of the photovoltaic device based on **TPA-BT-C8** and **TPA-3Th**. Both **TPA-BT-C8** and **TPA-3Th** have a TPA group which mainly determines their HOMO energy level, so they have nearly equal HOMO energy level. In addition, since the electron-donor ability of trithiophene group in **TPA-3Th** is stronger than that of single thiophene group in **TPA-BT-C8**,

and they have some contribution to the HOMO energy level, the HOMO energy level of **TPA-3Th** is somewhat higher than that of **TPA-BT-C8**. The electron-acceptor ability of benzothiadiazole and 2-(5,5-dimethylcyclohex-2-en-1-ylidene)malononitrile (DCM) groups in **TPA-BT-C8** are a little stronger than that of cyano-*n*-octyl acetate in **TPA-3Th**, resulting in that **TPA-BT-C8** has a somewhat lower LUMO energy level than **TPA-3Th**.

### Theoretical calculation

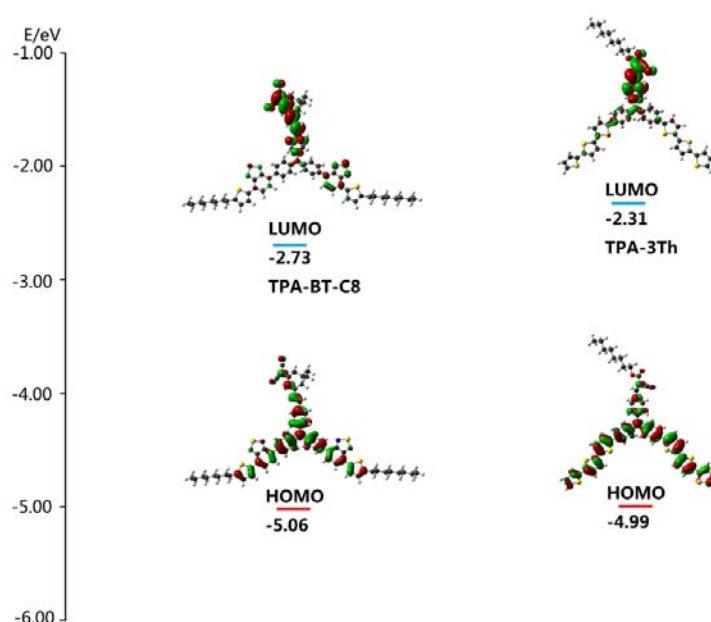


**Fig. 4** HOMO and LUMO pictograms and corresponding energy levels of **TPA-BT-C8** and **TPA-3Th** obtained at B3LYP/6-31G\* level.

The ground-state geometry and electron-state-density distribution of the HOMO and LUMO energy levels of **TPA-BT-C8** and **TPA-3Th** have been fully optimized using density functional theory (DFT) based on the B3LYP method with a 6-31G\* basis in Gaussian 03 program package. The HOMO and LUMO pictograms and corresponding energy levels for **TPA-BT-C8** and **TPA-3Th** are presented in Fig 4. The calculation results demonstrate that the HOMO energy level of **TPA-BT-C8**

distributes mainly on the triphenylamine core with some extending to the symmetrical two arms, and the LUMO energy level distributes on the acceptor groups, DCM and benzothiadiazole groups. However, as to **TPA-3Th**, the HOMO energy level distributes on the triphenylamine core and the six thiophene groups, and the LUMO energy level distributes only on the cyano-n-octyl acetate group. The DFT calculation indicated that ICT absorption can take place in both of **TPA-BT-C8** and **TPA-3Th**, but the intensity of **TPA-BT-C8** should be stronger than that of **TPA-3Th**, which accords with their optical properties. The calculated HOMO, LUMO energy levels and the band gap of **TPA-BT-C8** are -5.06, -2.73 and 2.33 eV, and as to **TPA-3Th**, they are -4.99, -2.31 and 2.68 eV, respectively. In general, the theoretical HOMO energy levels of **TPA-BT-C8** and **TPA-3Th** are consistent with those obtained from electrochemical measurement, and the trend of theoretical band gaps agrees with that of optical band gaps. The differences between the theoretical and electrochemical and optical values are a well-known consequence of performing calculations that lack medium-related factors.

### Photovoltaic properties

Bulk heterojunction photovoltaic cells with a device structure of glass/ITO/PEDOT:PSS/ **TPA-BT-C8** or **TPA-3Th**:PCBM/LiF/Al were fabricated and their performances were measured under a simulated AM1.5G illumination of  $100 \text{ mW cm}^{-2}$ . The current density-voltage characteristics of the devices are illustrated in Fig. 5. The optimized conditions and photovoltaic parameters for the devices are summarized in Table 2. Both of the two devices achieve the best

performance at a weight blend ratio of 1:2.5. The device based on **TPA-BT-C8** shows an optimal performance with a  $V_{oc}$  of 0.91 V, a  $J_{sc}$  of  $8.47 \text{ mA cm}^{-2}$ , a fill factor (FF) of 0.30 and

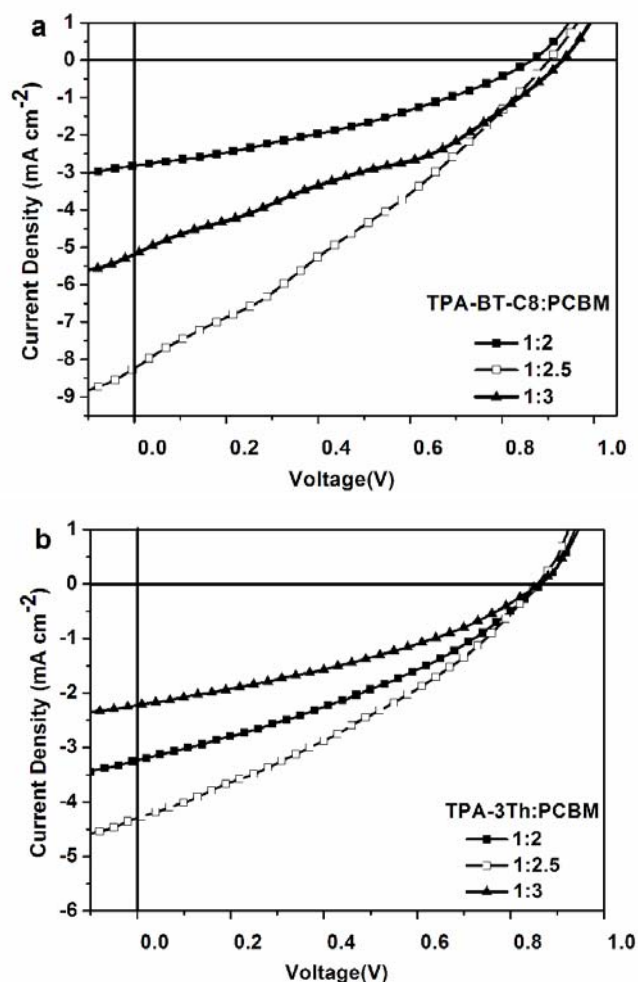
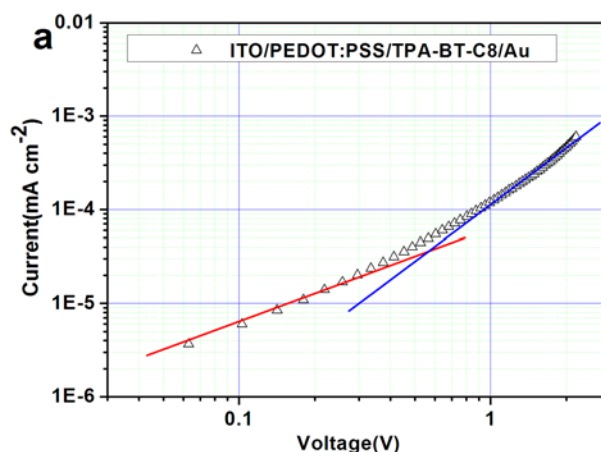


**Fig. 5** The current-voltage (J-V) curves of the solar cells based on TPA-BT-C8 or TPA-3Th:PCBM with varying blend ratios under simulated AM1.5 solar illumination ( $100 \text{ mW cm}^{-2}$ ).

**Table 2** Photovoltaic parameters of the solar cells based on TPA-BT-C8 or TPA-3Th:PCBM under simulated AM1.5 solar illumination ( $100 \text{ mW cm}^{-2}$ ).

Molecule	Small molecule:PCBM (w:w ratio)	$V_{oc}$ (V)	$J_{sc}$ ( $\text{mA cm}^{-2}$ )	FF	PCE (%)
<b>TPA-BT-C8</b>	1:2	0.86	2.75	0.37	0.88
<b>TPA-BT-C8</b>	1:2.5	0.91	8.47	0.30	2.26
<b>TPA-BT-C8</b>	1:3	0.93	5.04	0.36	1.68
<b>TPA-3Th</b>	1:2	0.87	3.26	0.35	0.98
<b>TPA-3Th</b>	1:2.5	0.86	4.32	0.34	1.21
<b>TPA-3Th</b>	1:3	0.86	2.29	0.35	0.69

a PCE of 2.26%. The device based on **TPA-3Th** exhibits its best performance with a  $V_{oc}$  of 0.86 V, a  $J_{sc}$  of  $4.32 \text{ mA cm}^{-2}$ , a FF of 0.34 and a PCE of 1.21%. The much higher PCE of **TPA-BT-C8** based device than that of **TPA-3Th** based device is resulted from the higher  $J_{sc}$ , 8.47 vs.  $4.32 \text{ mA cm}^{-2}$ , and this is mainly attributed to the much wider solar light absorption of **TPA-BT-C8** than **TPA-3Th** (see Fig. 2). The somewhat higher  $V_{oc}$  of the device based on **TPA-BT-C8** (0.91 V) than that of the device based on **TPA-3Th** (0.86 V) is consistent with their HOMO energy levels obtained from electrochemical measurement and DFT theoretical calculation, which is -5.38 eV vs. -5.35 eV by electrochemical measurement and -5.06 eV vs. -4.99 eV by DFT theoretical calculation (vide ut supra), since  $V_{oc}$  of the bulk heterojunction photovoltaic cells is mainly determined by the difference between HOMO energy level of the donor and LUMO energy level of the acceptor.<sup>1d</sup>



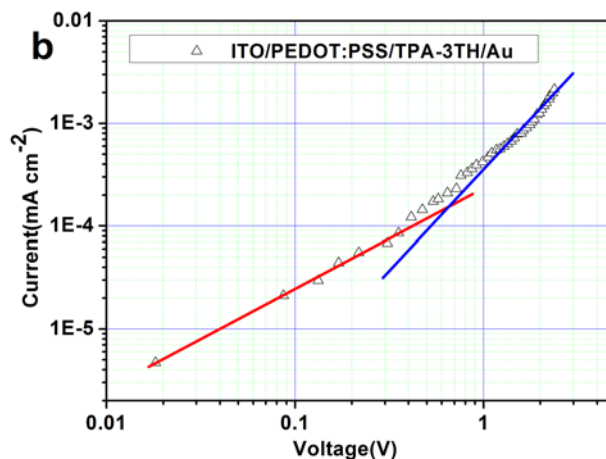


**Fig. 6**  $J$ - $V$  curves in the dark of ITO/PEDOT:PSS/TPA-BT-C8 or TPA-3Th/Au devices in log axis for estimating the hole mobility of TPA-BT-C8 (a) and TPA-3Th (b). The thicknesses of TPA-BT-C8 or TPA-3Th films are around 70 nm. The open triangle symbols are the experimental data. The solid line from 0.02 to 0.6 V means  $\log J$  is fitted linearly dependent on  $\log V$  with a slope of 1. The solid line from 0.6 to 1 V means  $\log J$  is fitted linearly dependent on  $\log V$  with a slope of 2 (SCLC area).

Charge carrier mobility of materials is another important factor to influence the performance of OSCs. Accordingly, we investigated the hole mobility of TPA-BT-C8 and TPA-3Th by space charge limited current (SCLC) method.<sup>18</sup> Devices with a structure of ITO/TPA-BT-C8 or TPA-3Th/LiF/Al were fabricated and their J-V curves in the dark are shown in Fig. 6. The hole mobility of TPA-BT-C8 and TPA-3Th was estimated according to the following equation:

$$J = \frac{9}{8} \varepsilon_r \varepsilon_0 \mu_h \frac{(V - V_{bi})^2}{L^3}$$

Where  $V$  is the applied voltage, and  $J$  is the current density.  $\varepsilon_r$  and  $\varepsilon_0$  are the relative dielectric constant (Here we fit it to be 3.) and the permittivity of the vacuum ( $8.85 \times 10^{-12}$  F m<sup>-1</sup>), respectively.  $\mu_h$  is hole mobility and  $L$  is the thickness of organic layer.  $V_{bi}$  is fitted to be about 0.1 V, which is determined by the difference between the work functions of the cathode and anode. Then the hole mobility of TPA-BT-C8

and **TPA-3Th** is estimated to be  $7.1 \times 10^{-5}$  and  $1.6 \times 10^{-4} \text{ cm}^2 \text{ V}^{-1} \text{ s}^{-1}$ , respectively. Both of the two small molecules have a relatively high hole mobility, which is favorable for performance of the photovoltaic cell. On the other hand, the hole mobility of **TPA-3Th** is higher than that of **TPA-BT-C8**, but the performance of the photovoltaic cell based on **TPA-BT-C8** is better than that of the photovoltaic cell based on **TPA-3T**. We think this is because the hole mobility of the donor materials is not the dominant factor to influence the performance of these two devices. Just as we analyzed above, the much wider solar light absorption of **TPA-BT-C8** than **TPA-3Th** is an important factor that can't be ignored.

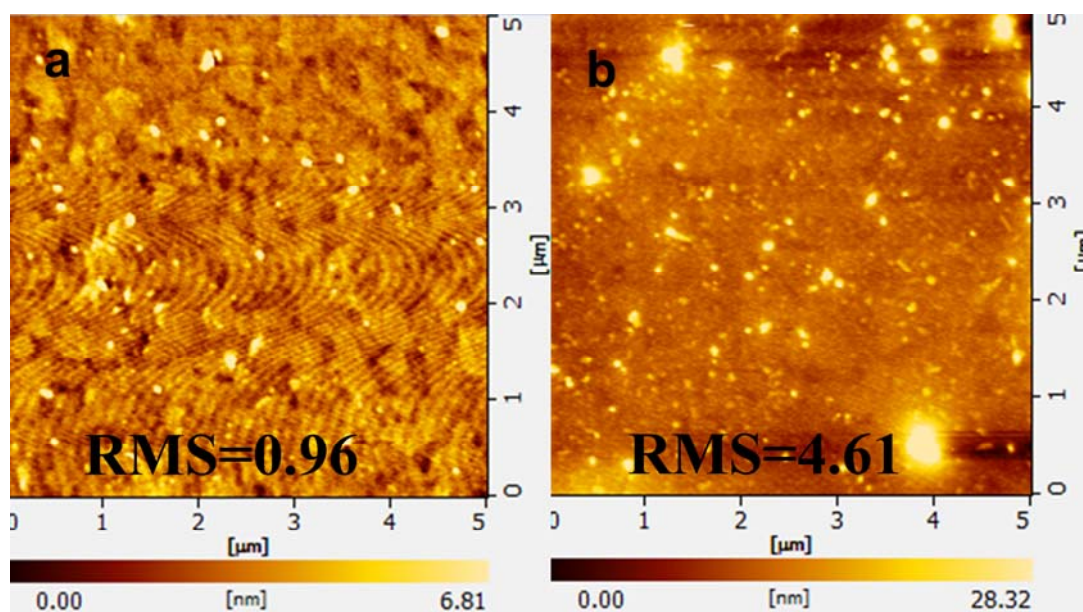


**Fig. 7** AFM Topography images (size  $5 \mu\text{m} \times 5 \mu\text{m}$ ) of **TPA-BT-C8:PCBM** (1:2.5) (a) and **TPA-3Th:PCBM** (1:2.5) (b) films.

To further investigate the reason why the photovoltaic performance of device based on **TPA-BT-C8** is much better than that of device based on **TPA-3Th**, morphology of their active layers was investigated by AFM. As demonstrated in Fig. 7, many large aggregates with several hundreds of nanometers can be found in the

**TPA-3Th**:PCBM blend film, while the surface of **TPA-BT-C8**:PCBM blend film looks like much smooth. In addition, the root mean square (rms) roughness of **TPA-BT-C8**:PCBM blend film is much lower than that of **TPA-3Th**:PCBM blend film, which is 0.96 and 4.61, respectively. Therefore, **TPA-BT-C8** has a better compatibility and film-formation property with PCBM than **TPA-3Th**, and this partially leads to that the photovoltaic device based on **TPA-BT-C8** has a higher  $J_{sc}$  and PCE than the device based on **TPA-3Th**.

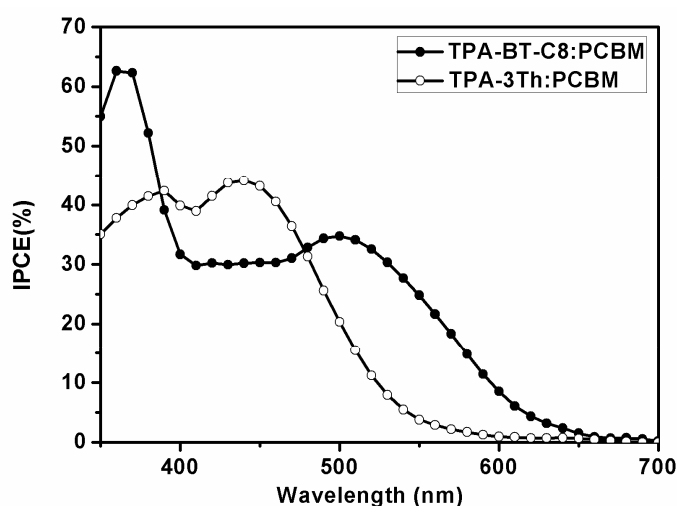


**Fig. 8** IPCE curves of the OSCs devices based on **TPA-BT-C8** or **TPA-3Th**:PCBM (1:2.5).

Fig. 8 shows the IPCE curves of photovoltaic devices based on **TPA-BT-C8**:PCBM (w:w, 1:2.5) and **TPA-3Th**:PCBM (w:w, 1:2.5). It was found that IPCE spectra of the devices are basically consistent with the UV-vis absorption spectra of **TPA-BT-C8** and **TPA-3Th**. The device based on **TPA-BT-C8**:PCBM has a wider response range than the device based on **TPA-3Th**:PCBM. More importantly, the response range of **TPA-3Th**:PCBM based device is mainly between 350 to 530 nm, while that of **TPA-BT-C8**:PCBM based device is extended from 350 to 630 nm

which is more close to the maximum photon flux of the solar irradiation at  $\sim 700$  nm,<sup>19</sup> and so **TPA-BT-C8**:PCBM based device has a stronger ability of absorbing photons than **TPA-3Th**:PCBM based device. Consequently, it is reasonable that the device based on **TPA-BT-C8** has a higher  $J_{sc}$  and PCE than the device based on **TPA-3Th**.

## Conclusions

In summary, two solution-processable two-dimensional conjugated organic small molecules, **TPA-BT-C8** and **TPA-3Th**, were synthesized successfully by Knoevenagel condensation reaction. For **TPA-BT-C8**, two arms of the TPA core are symmetrically connected with thiophene donor group and benzothiadiazole acceptor group, which brings about ICT and it makes **TPA-BT-C8** has a red-shifted and wider absorption than **TPA-3Th** whose two arms of TPA core are composed of only donor group, terthiophene. Both of the two molecules has a deep HOMO energy level, which ensures that the two molecules have a good air stability and the photovoltaic devices based on **TPA-BT-C8** or **TPA-3Th** has a high  $V_{oc}$  of about 0.9 V. The device based on **TPA-BT-C8** has a higher  $J_{sc}$  ( $8.47 \text{ mA cm}^{-2}$ ) and power conversion efficiency (PCE) (2.26%) than the device based on **TPA-3Th** ( $4.32 \text{ mA cm}^{-2}$ , 1.21%), resulting from the wider solar light absorption of **TPA-BT-C8** and good compatibility and film-formation ability of **TPA-BT-C8** with PCBM than **TPA-3Th**. The IPCE spectra also confirmed that the device based on **TPA-BT-C8** has a wider and red-shifted response range than the device based on **TPA-3Th**. The investigations indicate that the two-dimensional conjugated organic small molecules are a type of

promising organic photovoltaic materials, and offer a new strategy for designing organic small molecular solar cell materials.

### Acknowledgements

This work was supported by 973 program (2014CB643506), the Project Sponsored by the Scientific Research Foundation for the Returned Overseas Chinese Scholars, State Education Ministry, the Research Fund of Key Laboratory of Physics and Technology for Advanced Batteries, Ministry of Education (Grant no. 201206), and the Research Fund of State Key Laboratory of Inorganic Synthesis and Preparative Chemistry, Jilin University (Grant no. 2011-25).

### References

- 1 (a) G. Yu, J. Gao, J. C. Hummelen, F. Wudl and A. J. Heeger, *Science.*, 1995, **270**, 1789-1791; (b) C. J. Brabec, *Sol. Energ. Mat. Sol. C*, 2004, **83**, 273-292; (c) S. Gunes, H. Neugebauer and N.S. Sariciftci, *Chem. Rev.*, 2007, **107**, 1324-1338; (d) M. C. Scharber, D. Wuhlbacher, M. Koppe, P. Denk, C. Waldauf, A. J. Heeger and C. L. Brabec, *Adv. Mater.*, 2006, **18**, 789-794.
- 2 (a) J. Y. Zhou, X. J. Wan, Y. S. Liu, Y. Zuo, Z. Li, G. R. He, G. K. Long, W. Ni, C. X. Li, X. C. Su and Y. S. Chen, *J. Am. Chem. Soc.*, 2012, **134**, 16345-16351; (b) Y. M. Sun, G. C. Welch, W. L. Leong, C. J. Takacs, G. C. Bazan and A. J. Heeger, *Nat. Mater.*, 2012, **11**, 44-48; (c) T. S. van der Poll, J. A. Love, T. Q. Nguyen and G. C. Bazan, *Adv. Mater.*, 2012, **24**, 3646-3649; (d) Y. W. Li, Q. Guo, Z. F. Li, J. N. Pei and W. J. Tian, *Energ. Environ. Sci.*, 2010, **3**, 1427-1436.

- 3 (a) Z. Q. Jiang, T. L. Ye, C. L. Yang, D. Z. Yang, M. R. Zhu, C. Zhong, J. G. Qin and D. G. Ma, *Chem. Mater.*, 2011, **23**, 771-777; (b) Y. Shirota and Hiroshi Kageyama, *Chem. Rev.*, 2007, **107**, 953-1010; (c) Y. Shirota, *J. Mater. Chem.*, 2005, **15**, 75-93.
- 4 J. L. Wang, Z. C. He, H. B. Wu, H. B. Cui, Y. Li, Q. H. Gong, Y. Cao and J. A. Pei, *Chem.-Asian J.*, 2010, **5**, 1455-1465.
- 5 (a) N. Metri, X. Sallenave, C. Plesse, L. Beouch, P. H. Aubert, F. Goubard, C. Chevrot and G. Sini, *J. Phys. Chem C*, 2012, **116**, 3765-3772; (b) Y. Yang, J. Zhang, Y. Zhou, G. J. Zhao, C. He, Y. F. Li, M. Andersson, O. Inganäs and F. L. Zhang, *J. Phys. Chem. C*, 2010, **114**, 3701-3706; (c) G. J. Zhao, G. L. Wu, C. He, F. Q. Bai, H. X. Xi, H. X. Zhang and Y. F. Li, *J. Phys. Chem. C*, 2009, **113**, 2636-2642; (d) H. X. Shang, H. J. Fan, Y. Liu, W. P. Hu, Y. F. Li and X. W. Zhan, *Adv. Mater.*, 2011, **23**, 1554-1557.
- 6 (a) J. Zhang, D. Deng, C. He, Y. J. He, M. J. Zhang, Z. G. Zhang, Z. J. Zhang and Y. F. Li, *Chem. Mater.*, 2011, **23**, 817-822; (b) J. Zhang, Y. Yang, C. He, Y. J. He, G. J. Zhao and Y. F. Li, *Macromolecules*, 2009, **42**, 7619-7622.
- 7 (a) G. L. Wu, G. J. Zhao, C. He, J. Zhang, Q. G. He, X. M. Chen and Y. F. Li, *Sol. Energ. Mat. Sol. C*, 2009, **93**, 108-113; (b) J. Zhang, J. T. Yu, C. He, D. Deng, Z. G. Zhang, M. J. Zhang, Z. B. Li and Y. F. Li, *Org. Electron.*, 2012, **13**, 166-172; (c) C. He, Q. G. He, Y. P. Yi, G. L. Wu, F. L. Bai, Z. G. Shuai and Y. F. Li, *J. Mater. Chem.*, 2008, **18**, 4085-4090; (d) J. Zhang, Y. Yang, C. He, D. Deng, Z. B. Li and Y. F. Li, *J. Phys. D Appl. Phys.*, 2011, **44**, 475101 (5pp); (e) D. Deng, S. L.

- Shen, J. Zhang, C. He, Z. J. Zhang and Y. F. Li, *Org. Electron.*, 2012, **13**, 2546-2552.
- 8 (a) O. Alevéque, P. Leriche, N. Cocherel, P. Frere, A. Cravino and J. Roncali, *Sol. Energ. Mat. Sol. C.*, 2008, **92**, 1170-1174; (b) A. Cravino, S. Roquet, P. Leriche, O. Alevéque, P. Frere and J. Roncali, *Chem. Commun.*, 2006, 1416-1418; (c) S. Roquet, A. Cravino, P. Leriche, O. Alevéque, P. Frere and J. Roncali, *J. Am. Chem. Soc.*, 2006, **128**, 3459-3466. (d) E. Ripaud, T. Rousseau, P. Leriche and J. Roncali, *Adv. Energy Mater.*, 2011, **1**, 540-545.
- 9 (a) M. M. Stylianakis, J. A. Mikroyannidis, Q. F. Dong, J. N. Pei, Z. Y. Liu and W. J. Tian, *Sol. Energ. Mat. Sol. C.*, 2009, **93**, 1952-1958; (b) J. Cremer and P. Bauerle, *J. Mater. Chem.*, 2006, **16**, 874-884; (c) Y. Z. Lin, P. Cheng, Y. F. Li and X. W. Zhan, *Chem. Commun. Camb.*, 2012, **48**, 4773-4775; (d) D. Sahu, C. H. Tsai, H. Y. Wei, K. C. Ho, F. C. Chang and C. W. Chu, *J. Mater. Chem.*, 2012, **22**, 7945-7953; (e) S. L. Shen, L. Gao, C. He, Z. J. Zhang, Q. J. Sun and Y. F. Li, *Org. Electron.*, 2013, **14**, 875-881; (f) Z. Hu, X. D. Li, W. J. Zhang, A. H. Liang, D. D. Ye, Z. T. Liu, J. Liu, Y. J. Liu and J. F. Fang, *Rsc Adv.*, 2014, **4**, 5591-5597.
- 10 F. Huang, K. S. Chen, H. L. Yip, S. K. Hau, O. Acton, Y. Zhang, J. D. Luo and A. K. Y. Jen, *J. Am. Chem. Soc.*, 2009, **131**, 13886-13887.
- 11 (a) S. R. Marder, L. T. Cheng, B. G. Tiemann, A. C. Friedli, M. Blancharddesce, J. W. Perry and J. Skindhoj, *Science*, 1994, **263**, 511-514; (b) S. Liu, M. A. Haller, H. Ma, L. R. Dalton, S. H. Jang and A. K. Y. Jen, *Adv. Mater.*, 2003, **15**, 603-607.
- 12 J. Roncali, P. Leriche and A. Cravino, *Adv. Mater.*, 2007, **19**, 2045-2060.

- 13 Z. G. Zhang, K. L. Zhang, G. Liu, C. X. Zhu, K. G. Neoh and E. T. Kang, *Macromolecules*, 2009, **42**, 3104-3111.
- 14 Z. F. Li, J. N. Pei, Y. W. Li, B. Xu, M. Deng, Z. Y. Liu, H. Li, H. G. Lu, Q. A. Li and W. J. Tian, *J. Phys. Chem. C*, 2010, **114**, 18270-18278.
- 15 N. Kawahara, E. Tomita, A. Ohtsuki and Y. Aoyagi, *P. Combust Inst.*, 2011, **33**, 2903-2910.
- 16 (a) Z. Li, J. F. Ding, N. H. Song, J. P. Lu and Y. Tao, *J. Am. Chem. Soc.*, 2010, **132**, 13160-13161; (b) R. Cervima, X-C. Lz, G. W. C Spencer, A. B. Holmes, S. C. Moratti, R. H. Friend and *Synthetic Met.*, 1997, **84**, 359-369.
- 17 (a) P. T. Wu, F. S. Kim, R. D. Champion and S. A. Jenekhe, *Macromolecules*, 2008, **41**, 7021-7028; (b) B. C. Thompson, Y. G. Kim, T. D. McCarley and J. R. Reynolds, *J. Am. Chem. Soc.*, 2006, **128**, 12714-12725.
- 18 G. Yu, J. Gao, J. C. Hummelen, F. Wudl and A. J. Heeger, *Science*, 1995, **270**, 1789-1791.
- 19 R. Kroon, M. Lenes, J. C. Hummelen, P. W. M. Blom and B. De Boer, *Polym. Rev.*, 2008, **48**, 531-582.